ORIGINAL ARTICLE

TAZ promotes PDX1-mediated insulinogenesis

Mi Gyeong Jeong[1] · Hyo Kyeong Kim[1] · Gibbeum Lee[1] · Hee Yeon Won[1] · Da Hye Yoon[1] · Eun Sook Hwang[1]

Abstract

Transcriptional co-activator with PDZ-binding motif (TAZ) is a key mediator of the Hippo signaling pathway and regulates structural and functional homeostasis in various tissues. TAZ activation is associated with the development of pancreatic cancer in humans, but it is unclear whether TAZ directly affects the structure and function of the pancreas. So we sought to identify the TAZ function in the normal pancreas. TAZ defect caused structural changes in the pancreas, particularly islet cell shrinkage and decreased insulin production and β-cell markers expression, leading to hyperglycemia. Interestingly, TAZ physically interacted with the pancreatic and duodenal homeobox 1 (PDX1), a key insulin transcription factor, through the N-terminal domain of TAZ and the homeodomain of PDX1. TAZ deficiency decreased the DNA-binding and transcriptional activity of PDX1, whereas TAZ overexpression promoted PDX1 activity and increased insulin production even in a low glucose environment. Indeed, high glucose increased insulin production by turning off the Hippo pathway and inducing TAZ activation in pancreatic β-cells. Ectopic TAZ overexpression along with PDX1 activation was sufficient to produce insulin in non-β-cells. TAZ deficiency impaired the mesenchymal stem cell differentiation into insulin-producing cells (IPCs), whereas TAZ recovery restored normal IPCs differentiation. Compared to WT control, body weight increased in TAZ-deficient mice with age and even more with a high-fat diet (HFD). TAZ deficiency significantly exacerbated HFD-induced glucose intolerance and insulin resistance. Therefore, TAZ deficiency impaired pancreatic insulin production, causing hyperglycemia and exacerbating HFD-induced insulin resistance, indicating that TAZ may have a beneficial effect in treating insulin deficiency in diabetes.

Keywords Glucose homeostasis · Hippo · Insulin resistance · Prediabetes · Protein–protein interaction

Abbreviations

ChIP	Chromatin immunoprecipitation
FoxA2	Forkhead box A2
GCG	Glucagon
Glut	Glucose transporter
GSIS	Glucose-stimulated insulin secretion
GTT	Glucose tolerance test
HFD	High-fat diet
INS	Insulin
ITT	Insulin tolerance test
IPCs	Insulin-producing cells
KO	Knockout
LATS	Large tumor suppressor
MSC	Mesenchymal stem cell
MST	Mammalian sterile 20-like
NCD	Normal chow diet
NFAT	Nuclear factor of activated T cells
NR4A1	Nuclear receptor 4A1
PAX6	Paired box protein 6
PDX1	Pancreatic duodenal homeobox 1
P-KO	Pancreas-specific KO
PPARγ	Peroxisome proliferator-activated receptor γ
RUNX	Runt-related transcription factor
SI	Stimulation index
TAZ	Transcriptional co-activator with PDZ-binding motif
TEAD	TEA domain transcription factor
WT	Wild type
YAP	Yes-associated protein

✉ Eun Sook Hwang
  eshwang@ewha.ac.kr

[1] College of Pharmacy and Graduate School of Pharmaceutical Sciences, Ewha Womans University, C206 Science Building, 52 Ewhayeodae-Gil, Seodaemun-Gu, Seoul 03760, South Korea

Introduction

Transcriptional co-activator with PDZ-binding motif (TAZ) contains a WW domain, a coiled-coil domain, and a PDZ-binding motif and interacts with various transcription factors to regulate the transcription of target genes required for cell proliferation, differentiation, and survival [1, 2]. In adult mesenchymal stem cells (MSCs), TAZ interacts with runt-related transcription factor 2 (RUNX2), MyoD, and peroxisome proliferator-activated receptor γ (PPARγ) and reciprocally regulates musculoskeletal and adipose tissue regeneration [3]. TAZ is also important for maintaining renal and testicular structure and function through interaction with nuclear factor of activated T cells 5 (NFAT5) and nuclear receptor 4A1 (NR4A1) [4–6]. In particular, TAZ interacts with TEA domain transcription factor (TEAD), a key mediator of the highly conserved Hippo pathway [7, 8], and plays an important role in organ size control, liver regeneration, and colonic epithelial cell regeneration upon injury [9–11]. Moreover, TAZ–TEAD interaction promotes cancer cell proliferation, migration, and invasion [7, 8, 12]. Indeed, TAZ expression is markedly increased in human cancer, and its increased expression is closely associated with tumor aggressiveness and resistance to chemotherapy in breast and lung cancer [13–15]. Yes-associated protein (YAP), a TAZ homolog, also interacts with TEAD and sustains tumor growth, drug resistance, and malignancy [16]. Therefore, TAZ modulates cell-specific physiological functions in various cells and tissues and contributes to cell proliferation and migration of cancer cells via increased expression and sustained activation.

The pancreas plays key roles in regulating glucose homeostasis by releasing peptide hormones from the endocrine islet cells, including glucagon (GCG)-producing α-cells, insulin (INS)-producing β-cells, somatostatin (SMS)-producing δ-cells, ghrelin-producing ε-cells, and gastrin (GAS)-producing G-cells [17]. In particular, INS is synthesized and secreted by β-cells through regulation at the transcriptional and post-transcriptional/post-translational stages [18]. The *INS* gene promoter contains regulatory elements, including A1/A2/A3 boxes, C1 element, and E1/E2 boxes, and transcription factors such as pancreatic duodenal homeobox 1 (PDX1), MafA, and NeuroD1 bind to the *INS* gene promoter to enhance INS gene transcription [19]. The master transcription factor PDX1 is essential for early pancreatic development, β-cell maturation, and INS production [20, 21], and also increases the expression of mature β-cell markers Nkx6.1 and glucose transporter 2 (Glut2) [22, 23]. Interestingly, forkhead box A2 (FoxA2) and paired box protein 6 (PAX6), known as mature α-cell markers, are involved in the regulation of INS biosynthesis and secretion [24, 25]. More interestingly, there are increasing reports that the Hippo pathway modulates pancreatic function through regulation of β-cell survival, proliferation, and regeneration [26, 27]. While exogenous YAP expression in β-cells promoted cell proliferation without affecting INS production and the expression of β-cell markers, endogenous YAP inhibition enhanced the differentiation of stem cells into β-cells and improved INS production [28, 29]. In contrast, the Hippo ON state under diabetic conditions induces activation of large tumor suppressor (LATS) and mammalian sterile 20-like (Mst) kinases, YAP and TAZ upstream kinases, and causes β-cell apoptosis and dysfunction [27, 30]. Therefore, it is expected that TAZ may play a role in regulating pancreatic β-cell function similar to YAP. However, little is known about the TAZ function in the normal pancreas, except that TAZ expression is increased in pancreatitis and pancreatic cancer [31–33].

Table 1 Antibodies

Name	Supplier	Cat no	Clone no	Purpose
β-Actin	Santa Cruz Biotechnology	sc-47778	C4	IB
E-cadherin	BD Biosciences	610182	36/E-cadherin	IHC
Flag	Sigma-Aldrich	F7425		IB
Flag-M2	Sigma-Aldrich	A2220		IP
GCG	R&D	MAB1249	#181402	IHC
Glut2	R&D	MAB1440	#205115	IHC
INS	Santa Cruz Biotechnology	sc-9168	H-86	IHC
MYC	Santa Cruz Biotechnology	sc-40	9E10	IB and IP
PDX1	Cell Signaling	5679S	D59H3	IB, IHC, and ChIP
TAZ	Novus Biologicals BD Biosciences	NB 600-220 560235	M2-616	IB IHC and IP
TAZ/YAP	Cell Signaling Technology	#8418	D24E4	IB and IHC

IB immunoblot, *IHC* immunohistochemistry, *IP* immunoprecipitation

This study aimed to investigate the TAZ function in the pancreas and its underlying molecular mechanisms using pancreas-specific TAZ knockout (P-KO) mice.

Materials and methods

Materials

All tissue culture reagents were obtained from Hyclon (Logan, UT, USA), Gibco (Carlsbad, CA, USA), and Thermo Fisher Scientific (Waltham, MA, USA). Antibiotic G418 and puromycin were purchased from Sigma-Aldrich (St. Louis, MO, USA). Antibodies purchased are listed in Table 1.

Mouse model

Male wild-type (WT) C57BL/6 mice were purchased from the Jackson Laboratory (Minneapolis, MN, USA), and whole-body TAZ knockout (KO) mice were generated as previously reported [5]. Homozygous TAZ floxed mice were bred with the PDX1-cre or Prrx1-cre transgenic (Tg) mice (National Cancer Institute) to generate pancreas-specific TAZ KO (P-KO) and mesenchyme-specific TAZ KO (MSC-KO) mice. Genotyping primer sets are listed as follows: 5′-ctggactacatcttgagttgc-3′ and 5′-ggtgtacggtcag-taaatttg-3′ for PDX1-cre Tg; 5′-gcggtctggcagtaaaaactatc-3′ and 5′-gtgaaacagcattgctgtcactt-3′ for Prrx1-cre Tg; and TAZ-GP2, 5′-atgggacagtccgggag-3′, TAZ-GP3, 5′-gtgcaagtcagag-gagg-3′, and TAZ-ks-Neo-R, 5′-ggagaacctgcgtgcaatcca-3′ for TAZ-floxed mice. All mice were housed in a specific pathogen-free animal facility at Ewha Womans University.

Cell culture and establishment of stable cell clones

HEK293T (CRL-11268), mouse insulinoma NIT-1 (CRL-2055), and mesenchyme-like fibroblast C3H10T1/2 (CCL-226) cells were obtained from American Type Culture Collection (Manassas, VA, USA). HEK293T and C3H10T1/2 cells were maintained in Dulbecco's modified Eagle's medium (DMEM; Gibco) with 10% heat-inactivated fetal bovine serum (FBS; HyClone), and NIT-1 cells were maintained in Ham's F-12K (Thermo Fisher Scientific). Viral-producing Plat-E cells (Cell Biolabs Inc, San Diego, CA, USA) were cultured in DMEM, and rat insulinoma INS-1 cells (Merck, SCC208) were maintained in RPMI-1640 (Gibco) with 10% FBS, respectively. Viral-producing Plat-E cells were transfected with viral vectors (PDX1, TAZ, TAZ S4A, or shTAZ) and subsequently incubated in a 32℃ incubator for 24 h to obtain viral supernatants. C3H10T1/2,

MSC, NIT-1 cells, and INS-1 cells were incubated with viral supernatants and were selected in the presence of proper antibiotics (400 µg/ml G418 for PDX1 and 1 µg/ml puromycin for TAZ, TAZ S4A, or shTAZ), followed by maintenance under the same medium conditions.

Hematoxylin and eosin (HE) staining and immunohistochemistry (IHC)

Pancreatic tissue was isolated from male WT, TAZ KO, and TAZ P-KO mice (8–12 weeks of age or indicated separately) and fixed in 10% neutralized formalin. Paraffin-embedded tissue sections with a thickness of 4 µm were deparaffinized,

Table 2 Used primer sequences

| Primers for gene expression analysis		
Gene	Direction	Sequences
β-actin	Forward	5′-agagggaaatcgtgcgtgac-3′
	Reverse	5′-caatagtgatgacctggccgt-3′
FoxA2	Forward	5′-gccagcgagttaaagtatgc-3′
	Reverse	5′-tcatgttgctcacggaagag-3′
GAS	Forward	5′-aggatgcctcgactgtgtgtg-3′
	Reverse	5′-tgcttcttggacaggtctg-3′
GCG	Forward	5′-agcacgcccttcaagacac-3′
	Reverse	5′-aatcttgggcacggcgggag-3′
Glut2	Forward	5′-ggctaatttcaggactggtt-3′
	Reverse	5′-tttctttgccctgacttccct-3′
INS	Forward	5′-tcagagaccatcagcaagcag-3′
	Reverse	5′-gtctgaaggtccccgggggct-3′
MafA	Forward	5′-ttggaggagcgcttctcc-3′
	Reverse	5′-tctccagaatgtgccgctg-3′
Nkx6.1	Forward	5′-cccggagtgatgcagagtc-3′
	Reverse	5′-agaacgtgggtctggtgtgt-3′
PAX6	Forward	5′-cccatgcagatgcaaaagtc-3′
	Reverse	5′-aaagatggaagggcactccc-3′
PDX1	Forward	5′-agagcccaaccgcgtccagc-3′
	Reverse	5′-aacatcactgccagctccacc-3′
SMS	Forward	5′-tccgagcccaaccagacagag-3′
	Reverse	5′-agaagaagttcttgcagccag-3′
TAZ	Forward	5′-gtcaccaacagtagctcagatc-3′
	Reverse	5′-agtgattacagccaggttagaaag-3′
Biotin-labeled primers for DNA pulldown assay		
INS promoter	Forward	5′-biotin-ccaagggacatcaatattagg3′
	Reverse	5′-ctggtcactaagggctgggggg-3′
ChIP-qPCR primers of insulin and pdx1 promoter		
INS promoter	Forward	5′-actggttcatcaggccatc-3′
	Reverse	5′-tcctctctgcccccctggac-3′
Pdx1 promoter	Forward	5′-aggaggcagggtacctccag-3′
	Reverse	5′-agaaggcctctgagataccc-3′
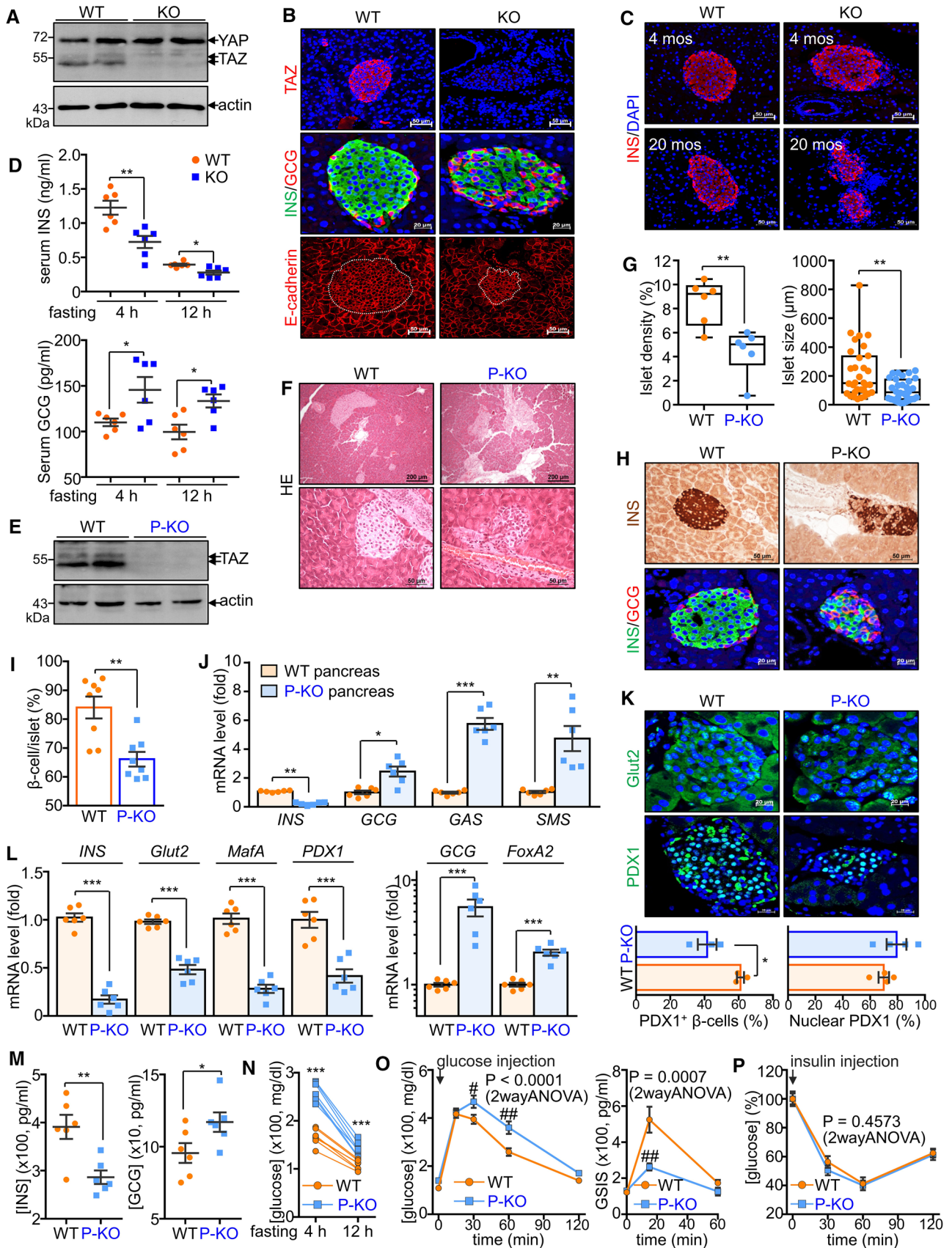
◄**Fig. 1** Impaired pancreatic structure and function in TAZ deficiency. (**A−D**) WT and whole-body TAZ KO mice (male, 12–16 weeks old or 20 months old, $n=6$ per group) were killed, and pancreatic tissue was obtained. Protein extracts were harvested from pancreatic tissue and analyzed by immunoblot assay with an antibody against TAZ/ YAP (**A**). Pancreatic tissue sections were stained with antibodies against TAZ, INS, GCG, or E-cadherin (**B**). Pancreatic tissue sections were prepared from WT and TAZ KO mice at 4 and 20 months of age and subjected to insulin immunostaining (**C**). Blood samples were collected from WT and TAZ KO mice after fasting for 4 or 12 h and used for ELISA to determine serum INS and GCG levels (**D**). **E−N** Pancreas-specific TAZ deleted (TAZ P-KO) mice (male, 12–16 weeks old, $n=6$ per group) were analyzed compared to littermate control mice (male, $n=6$). Protein extracts of the pancreas were obtained and analyzed by immunoblot assay with anti-TAZ antibody (**E**). Pancreatic tissue sections were subjected to HE staining (**F**). Islet density per unit area of the pancreas and various islet sizes were quantitated analyzed in WT and TAZ P-KO mice (**G**). Pancreatic tissues were stained with antibodies against INS or GCG, followed by detection with DAB or fluorescence (**H**). INS-positive β-cells were determined in five islets of WT and TAZ P-KO mice ($n=8$ per group) (**I**). Total RNA was obtained from the pancreas of WT and TAZ P-KO mice, the relative transcript levels of *INS*, *GCG*, *GAS*, and *SMS* were determined by quantitative real-time PCR (**J**). Pancreatic islets of WT and TAZ P-KO mice were stained with an antibody against GLUT2 and PDX1. PDX1-positive INS-producing cells and nuclear PDX1 levels were compared between WT and TAZ P-KO ($n=3$–4, **K**). Pancreatic islet cells were isolated from the WT and TAZ P-KO pancreas and subjected to quantitative real-time PCR analysis of *INS*, *GLUT2*, *MAFA*, *GCG*, and *FOXA2* (**L**). Blood samples were obtained from WT and TAZ P-KO mice after 4 and 12 h fasting for measuring serum INS and GCG, respectively (**M**). Blood glucose levels were determined at 4 and 12 h after fasting (**L**). WT and TAZ P-KO mice were intraperitoneally injected with glucose (1.5 g/kg, **M**), and blood samples were subjected to GTT and GSIS assays (**O**). For ITT assay, WT and TAZ P-KO mice were injected with insulin (0.75 U/ kg) (**P**). DAPI stained nuclei in **B**, **C**, **H**, and **K**. Representative image is from at least three independent experiments, and data are expressed as the means ± SEM from three to eight independent experiments. *$P<0.05$; **$P<0.005$; ***$P<0.0005$ by two-tailed Student's t test. #$P<0.05$; ##$P<0.01$ by 2wayANOVA with post hoc Tukey's multiple comparisons

rehydrated, incubated in 1% hydrochloric acid, and washed with distilled water. Tissue sections were stained with HE staining solution (Sigma-Aldrich) and observed under a Nikon Eclipse E200 microscope (Nikon, Japan). For IHC analysis, tissue slides were incubated with primary antibody followed by fluorescence-conjugated secondary antibody (Molecular Probes, Eugene, OR, USA). Cell nuclei were stained with 4, 6-diamidino-2-phenylindole (DAPI, Sigma-Aldrich). Cell images were observed with a confocal microscope (Nikon A1R, Nikon; LSM880 with Airyscan, Zeiss at Ewha Drug Development Research Core Center). Islet density (the number of islets per defined area), size, and β-cell mass were determined as previously reported [34].

Glucose-stimulation insulin secretion (GSIS) assay

For in vivo GSIS assay, mice were intraperitoneally injected with glucose (2 g/kg) after overnight fasting. Blood samples were collected at 0, 15, and 60 min after glucose stimulation. Plasma samples were immediately obtained by centrifugation and subjected to ELISA. For in vitro GSIS assay, islet cells or differentiated IPCs were preincubated in glucose-free Krebs buffer for 2 h and stimulated with either 5 mM or 25 mM glucose for 1 h. Secreted INS levels into supernatants were assessed by ELISA [35].

Enzyme-linked immunosorbent assay (ELISA)

According to the manufacturer's instructions, INS level was measured using a mouse INS ELISA kit (sensitivity 39 pg/ml, #ARKIN-011T, Fujifilm Wako Shibayagi Corp., Japan). Briefly, 96-well plates pre-coated with anti-INS antibody were washed and incubated with serum or culture supernatants, followed by biotin-conjugated anti-INS antibody and horseradish peroxidase enzyme-conjugated streptavidin. The plates were incubated with a substrate chromogen reagent after washing and measured at 450 nm. A serial dilution series of standard INS solutions were used for a standard calibration curve. A mouse GCG ELISA assay was performed by incubating GCG conjugates and substrate solution in the antibody pre-coated plate following the manufacturer's instructions (sensitivity 14.7 pg/ml, DGCGO, GCG standard Quantikine ELISA kit, R&D Systems).

Reverse transcription (RT) and real-time polymerase chain reaction (PCR)

Total RNA was isolated from mouse pancreas, primary pancreatic islet cells, INS-1, and NIT-1 cells using TRIzol reagent and subjected to RT using a cDNA synthesis kit (Thermo Fisher Scientific). Real-time PCR was performed in triplicate using StepOnePlus (Applied Biosystems, Foster City, CA, USA), and the average C_t value was used in the analysis. The relative expression level was calculated after normalization to the β-actin level using the $2^{-\Delta\Delta Ct}$ method [36]. The primer sets are listed in Table 2.

Intraperitoneal glucose tolerance test (GTT) and INS tolerance test (ITT)

The GTT and ITT assays were conducted as previously reported [37, 38]. In brief, for the GTT assay, all mice were fasted overnight and injected intraperitoneally with glucose
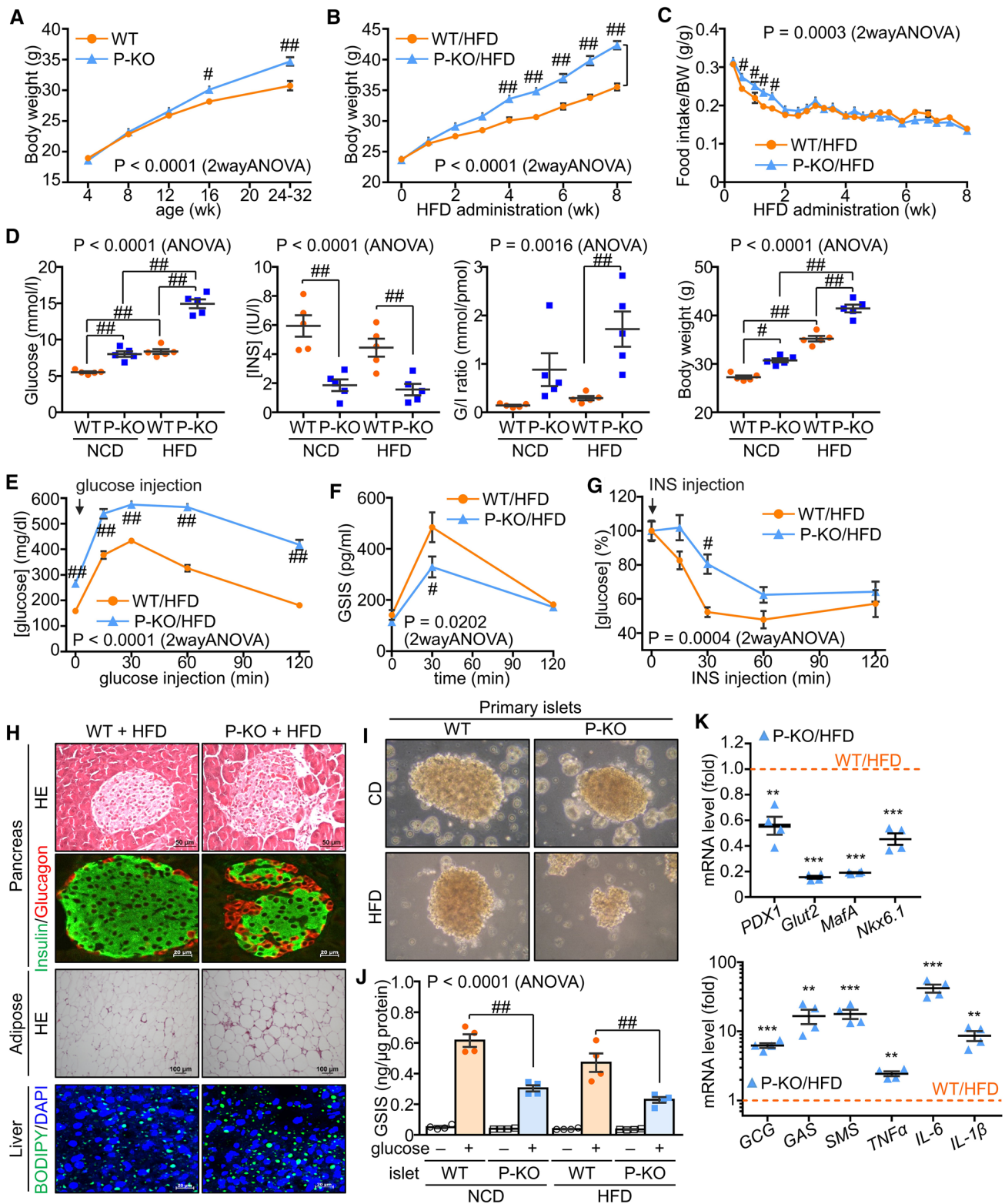
solution (1.5 g/kg). Blood samples were taken from tail veins at 0, 15, 30, 60, and 120 min, and blood glucose levels were measured using a glucometer (AccuCheck, Roche Diagnostics, GmbH Mannheim, Germany). Separately, mice were fasted for 4 h for the ITT assay and injected with regular human INS (0.75 U/kg Humulin-R, Eli Lilly). Blood samples were obtained at 0, 30, 60, and 120 min and analyzed using a glucometer.

◄**Fig. 2** Exacerbation of glucose intolerance and insulin resistance in HFD-fed TAZ P-KO. **A** Age-dependent body weight changes in WT and TAZ P-KO mice ($n=6$ per group) fed a normal chow diet (NCD). **B–K** WT and TAZ P-KO mice (males, 8 weeks old, $n=5$–8 per group) were fed an HFD for up to 8 weeks and killed for further analysis. Bodyweight (**B**) and food intake (**C**) were monitored in HFD-fed WT and TAZ P-KO mice ($n=6$ in **B**; $n=5$ in **C**). WT and TAZ P-KO mice (8 weeks old, $n=5$ per group) were fed NCD or HFD for 8 weeks and monitored weight gain, followed by fasting overnight. Blood glucose and INS levels, HOMA, and the fasting glucose to insulin ratio were determined in NCD- or HFD-fed WT and TAZ P-KO mice (**D**). HFD-fed WT and TAZ P-KO mice were injected with glucose and subjected to GTT (**E**) and GSIS assays (**F**). Separately, mice were injected with INS, followed by blood glucose measurement (**G**) ($n=6$ in **E** and **F**; $n=8$ in **G**). Pancreatic, adipose, and liver tissues were prepared from HFD-fed mice ($n=3$ per group) and subjected to HE staining, immunohistochemistry, or BODIPY staining (**H**). Pancreatic islet cells were isolated and cultured for 3 days (**I**) ($n=4$ per group). Islet cells were stimulated with glucose (25 mM) for 1 h for GSIS assay (**J**) ($n=4$ per group). Cells were cultured under high glucose (25 mM) conditions for 12 h and subjected to quantitative real-time PCR ($n=4$ per group). Gene expression levels were calculated relative to the WT control (set to 1 in WT) (**K**). Data are expressed as the mean ± SEM. $^{\#}P<0.05$; $^{\#\#}P<0.01$ by 2wayANOVA with Tukey's multiple comparisons or ANOVA with Tukey's HSD test. $^{**}P<0.005$; $^{***}P<0.0005$ by two-tailed Student's t test

HFD administration and lipid staining

Male WT and TAZ P-KO mice (8 weeks of age) were fed HFD (~ 60% of kcals from fat, Research Diets D12492, NJ, USA) for 8 weeks, and HFD food intake and body weight changes were continuously monitored for 8 weeks. After 8 weeks, blood samples were collected for measuring glucose, INS, and GCG. Separately, mice were subjected to blood glucose measurement for the GTT assay, ITT assay, and isolation of pancreatic islet cells. Liver and adipose tissues were isolated and immediately placed on a mold filled with sufficient OCT compound (Sigma-Aldrich), followed by freezing in liquid nitrogen. Frozen liver tissue slides were stained with BODIPY 493/503 staining solution, which stains neutral lipids (Thermo Fisher Scientific), and analyzed using a fluorescence microscope and Nikon confocal microscope. Adipose tissue was stained with HE staining solution, followed by observation with a microscope.

Isolation and cultivation of the pancreatic islets

Pancreatic islets were isolated from the pancreas of WT and TAZ P-KO mice by incubation with collagenase P (0.8 mg/ml, Roche Diagnostics). Pancreatic cell aggregates were washed and filtered with a tissue-collecting sieve (400 μm, pluriSelect Life Science, Leipzig, Germany). Pancreatic islet cells were isolated and purified on Histopaque (Sigma-Aldrich) density gradients [39]. Primary pancreatic islet cells were cultured in RPMI-1640 (Gibco) supplemented with 10% FBS (GenDEPOT, Barker, TX, USA) for 2 days, and culture supernatants were collected to measure INS and GCG levels by ELISA.

Protein–protein interaction and DNA pulldown assay

HEK293T cells were transfected with various PDX1 and TAZ expression vectors using a calcium phosphate transfection method [40]. Total cell lysates were harvested in lysis buffer (20 mM Tris, pH 7.5, 0.5% Triton X-100, 2 mM MgCl$_2$, 1 mM DTT, and protease inhibitors). For protein–protein interaction assay, total cell lysates were incubated with a specific antibody and subsequently protein A/G-agarose beads, followed by immunoblot analysis. For DNA pulldown assay, cell lysates were obtained in HKMG buffer [5] and incubated with biotinylated double-stranded INS promoter DNA and subsequently streptavidin-agarose beads. The DNA–protein complex was further analyzed by immunoblot assay. Insulin promoter DNA (200 bp) was prepared by PCR using biotinylated forward and reverse primer sets in Table 2 and purification with a QIAquick gel extraction kit (Qiagen, Hilden, Germany).

Reporter assay

Highly transfectable HEK293T, NIT-1, and C3H10T1/2 cells were transiently transfected with the reporter gene (p*INS*-luc or p*GCG*-luc) and PDX and TAZ expression vectors via a calcium transfection method. The pCMVβ vector was also transfected to normalize the transfection efficiency. Cell lysates were harvested and subjected to luciferase assay (Promega, Madison, WI, USA) and β-galactosidase assay (Thermo Fisher Scientific). The relative luciferase activity was determined after normalization with β-galactosidase activity and is expressed as fold change compared with the control.
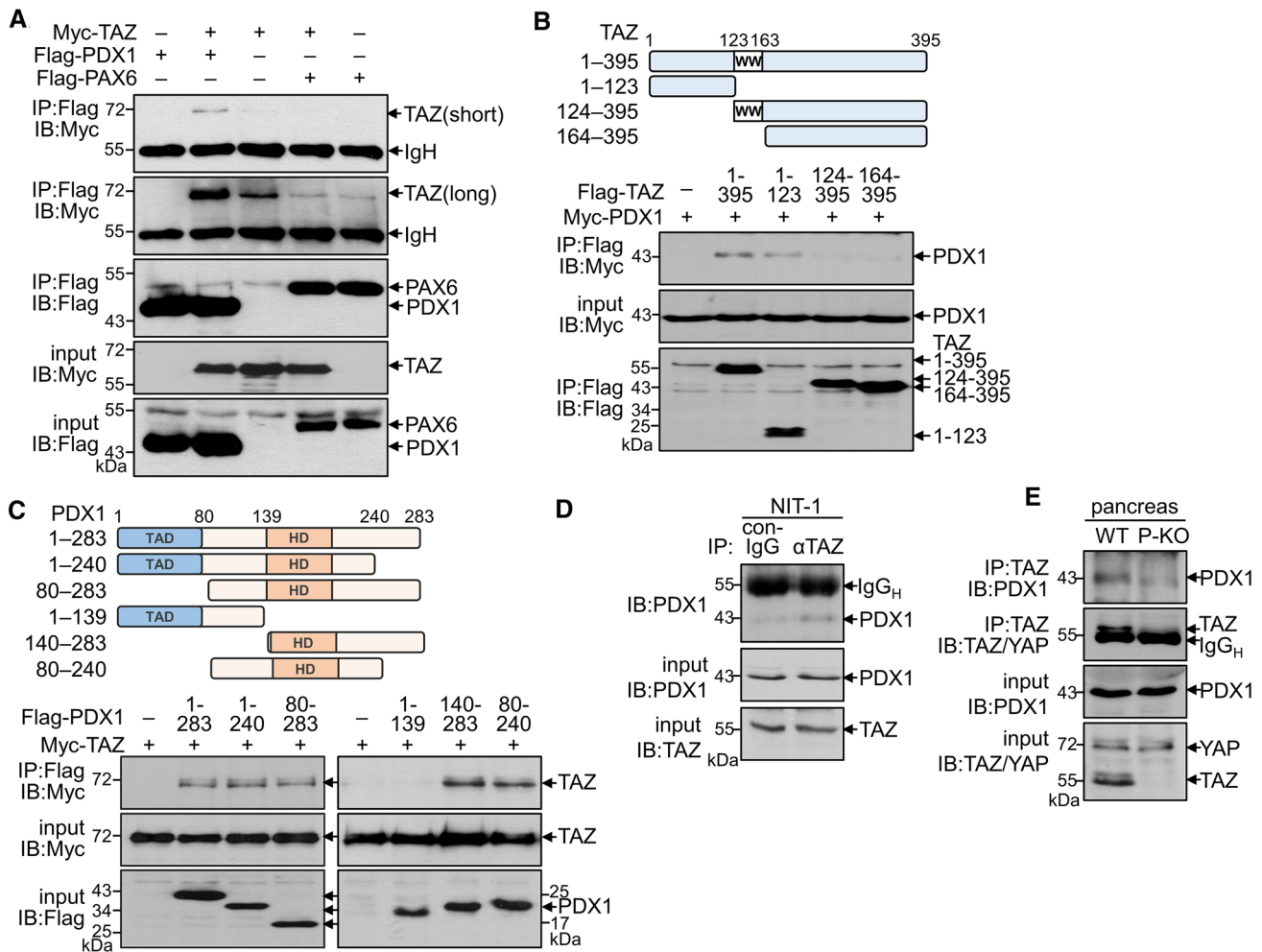
Fig. 3 Physical interaction between TAZ and PDX1. **A** Highly transfectable HEK293T cells were transfected with the expression vector of 6xMyc-tagged TAZ, Flag-tagged PDX, or Flag-tagged PAX6 and harvested. Protein extracts were incubated with anti-Flag antibody for immunoprecipitation, and the immune complexes were analyzed by immunoblot analysis. **B** HEK293T cells were transfected with the expression vector of TAZ truncations and PDX1 vector and subjected to immunoprecipitation and immunoblot analysis. **C** HEK293T cells were transfected with the expression vector of Flag-tagged PDX1 truncations and 6xMyc-TAZ vector, followed by immunoprecipitation and immunoblot analysis. **D** Protein extracts were harvested from NIT-1 cells and incubated with anti-TAZ antibody or control IgG antibody, followed by immunoblot analysis of PDX1. **E** Protein extracts were obtained from the pancreas of WT and TAZ P-KO and subjected to immunoprecipitation and immunoblot analysis. A representative image out of three independent experiments is presented

Chromatin immunoprecipitation (ChIP) assay

Stable NIT-1 cells (con/NIT-1 and TAZ/NIT-1) were expanded in the presence of puromycin and incubated with high glucose (25 mM) for 24 h. Cells were harvested, treated with 1% formaldehyde for 10 min, and subjected to a ChIP assay using a Magna ChIP™ A/G Chromatin Immunoprecipitation kit (Merck Millipore, Darmstadt, Germany). Cell lysates were sonicated to shear DNA and subsequently incubated with anti-PDX1 antibody and protein A/G magnetic beads. After washing, chromatin DNA

was eluted in ChIP elution buffer containing proteinase K and used for quantitative real-time PCR analysis and semi-quantitative PCR analysis [6]. The primers for *INS* and PDX1 genes are listed in Table 2.

Differentiation of MSCs and stable C3H10T1/2 cells into INS-producing cells (IPCs)

Bone marrow cells were collected from the femurs and tibias of WT, TAZ KO, prrx1-cre Tg (MSC-WT), and prrx1-cre TAZ KO (MSC-KO) mice and cultured in complete DMEM

for 3 days by discarding the non-adherent cells. MSCs were cultivated and expanded for an additional 3 days. To restore TAZ in TAZ-deficient MSCs, TAZ KO MSCs were infected with viral supernatants expressing mock or TAZ. Differentiation of IPCs from MSCs and stable C3H10T1/2 cells was performed with a few modifications according to the reported three-stage methods [41, 42]. Cells were grown to confluent in high glucose DMEM supplemented with 2% B27 for the first 2 days. Cells were then cultured in differentiation-conditioned medium containing nicotinamide (10 mM, Sigma-Aldrich), basic fibroblast growth factor (10 ng/ml, Peprotech, Rocky Hill, NJ, USA), epidermal growth factor (10 ng/ml, Peprotech), and B27 (2%, Thermo Fisher Scientific) for an additional 10–14 days by replacing the medium every other day. Cells were harvested to obtain total RNA, and culture supernatants were collected for measuring INS secretion.

Statistical analysis

All in vitro experiments were performed at least three times, and data are expressed as the mean ± standard error of the mean (SEM). The results were analyzed using one-way ANOVA (ANOVA) and the post hoc analysis with Tukey's HSD test, two-way ANOVA (2wayANOVA) with post hoc Tukey's multiple comparisons, or unpaired two-tailed Student's t test. P values less than 0.05 were considered statistically significant.

Results

TAZ deficiency in the pancreas induces structural and functional abnormalities and causes hyperglycemia

To determine whether TAZ is expressed in the pancreas and whether it modulates pancreatic functions, we compared the pancreatic tissue of WT and TAZ KO mice. TAZ was expressed in WT pancreas but not in TAZ KO mice, whereas YAP was equally expressed in WT and TAZ KO (Fig. 1A). TAZ was particularly expressed in the pancreatic islets, and its deficiency caused the architectural abnormalities in the endocrine and exocrine pancreas; decreased β-cells, increased and aberrant distribution of α-cells, and decreased E-cadherin expression (Fig. 1B). The decrease in INS-producing β-islet cells and alterations in islet architecture in TAZ KO mice were further exacerbated with ageing (Fig. 1C). Concurrently, serum INS was significantly decreased in TAZ KO mice in both 4 h- and 12 h-fasting conditions, and serum GCG levels were higher in TAZ KO than in WT control mice (Fig. 1D). To confirm the direct effects of TAZ deficiency in the pancreas, we generated

pancreas-specific TAZ KO (P-KO) mice and analyzed pancreatic phenotype compared to appropriate controls. Immunoblot analysis confirmed that TAZ expression was abolished in the TAZ P-KO pancreas (Fig. 1E). TAZ P-KO mice showed abnormal pancreatic structural alterations such as smaller and irregular islets and pancreatic epithelium destruction (Fig. 1F). The islet density and diameter were significantly lower in TAZ P-KO (Fig. 1G). In addition, INS-producing β-cells were decreased, and GCG-secreting α-cells were increased and aberrantly distributed in the pancreatic islets of TAZ P-KO mice (Fig. 1H). Likewise, the β-cell population per islet was reduced in TAZ P-KO (Fig. 1I). Furthermore, TAZ deficiency decreased INS expression but increased the expression of GCG, GAS, and SMS (Fig. 1J). The expression of GLUT2 and PDX1 proteins was also decreased in TAZ P-KO mice, and particularly PDX1-positive β-cells per islet were decreased by TAZ deficiency (Fig. 1K). Consistently, transcript levels of β-cell markers, including *INS*, *Glut2*, *MafA*, and *PDX1*, were substantially decreased in TAZ-deficient islet cells, while *GCG* and *FoxA2* mRNA levels were increased (Fig. 1L). Serum hormone analysis clarified that TAZ P-KO mice showed decreased INS levels and increased GCG levels (Fig. 1M). Furthermore, blood glucose levels in TAZ P-KO mice were significantly higher than in WT mice in fasting states (Fig. 1N). TAZ P-KO mice impaired glucose tolerance in response to glucose infusion due to defective INS production, and exogenous INS infusion controlled blood glucose to normal and similar levels in both WT and TAZ P-KO mice (Fig. 1O, P).

TAZ deficiency abnormally increases body weight with age and exacerbates glucose intolerance and INS resistance induced by a high-fat diet (HFD)

Since hyperglycemia is closely associated with the increasing prevalence of obesity, a major cause of INS resistance of type 2 diabetes, we assessed the effect of TAZ deficiency on body weight changes. TAZ P-KO mice tended to be overweight and obese with age under ad libitum conditions. The body weight of the WT and TAZ P-KO mice gradually increased with age, and the weight gain was significantly greater in TAZ P-KO mice than in WT control mice after 4 months of age (Fig. 2A). In addition, the weight gain induced by the HFD was significantly greater in TAZ P-KO mice than in WT mice despite the similar food intake (Fig. 2B, C). We compared blood glucose and INS levels between WT and TAZ P-KO after feeding a normal diet and HFD. Lack of INS in TAZ P-KO significantly increased blood glucose levels under both feeding conditions, consistent with weight gain. The G/I ratio was substantially increased in HFD-fed TAZ P-KO (Fig. 2D), suggesting the altered insulin sensitivity/resistance [43].
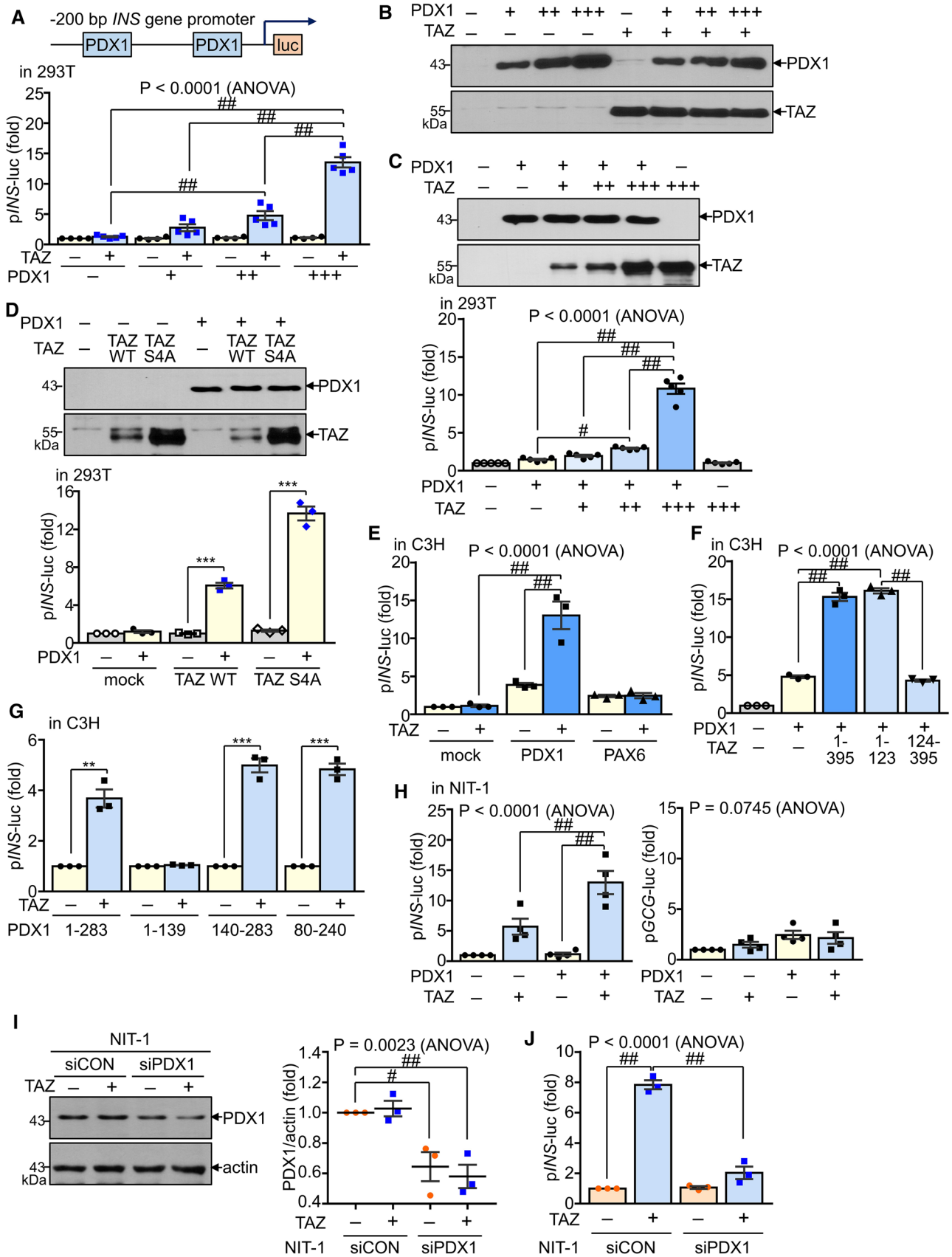
◄**Fig. 4** Facilitated *INS* promoter activity by the cooperation of PDX1 and TAZ. **A−D** HEK293T cells were transfected with the p*INS*-luc reporter gene together with PDX1 and TAZ expression vectors and subjected to reporter assay and immunoblot analysis. Schematic design of the insulin promoter reporter vector (p*INS*-luc) containing PDX1-binding elements. The p*INS*-luc promoter activity by PDX1 expression was determined in the absence or presence of TAZ (**A**). PDX1 and TAZ expressions were detected by immunoblot analysis (**B**). Dose-dependent effect of TAZ on the PDX1-mediated p*INS*-luc promoter activity and immunoblot assay of PDX1 and TAZ (**C**). Immunoblot analysis of TAZ WT, TAZ mutant (S4A), and PDX1. Effect of TAZ WT and TAZ S4A on the PDX1-induced p*INS*-luc reporter activity (**D**). **E−G** Mesenchymal C3H10T1/2 cells were transfected with various types of PDX1, PAX6, and/or TAZ together with pINS-luc and subjected to reporter assay. Cells were transfected with PDX1 or PAX6 expression vector with or without TAZ vector (**E**). Cells were transfected with PDX1 expression vector with TAZ truncations (**F**) or PDX1 truncations in the presence or absence of TAZ (**G**). **H−J** NIT-1 β-cells were transfected with either p*INS*-luc or p*GCG*-luc with PDX and TAZ expression vector and subjected to reporter assay (**H**). NIT-1 cells were transfected with siPDX1 and transiently transfected with TAZ expression vector and p*INS*-luc. Endogenous PDX1 expression after transfection with siPDX1 was analyzed by immunoblot analysis and quantitatively analyzed using Image J (**I**). Cells were transfected with p*INS*-luc together with siPDX1 and TAZ expression vector, and the *pINS*-luc promoter activity was assayed at 48 h (**J**). All experiments were conducted at least three times, and a representative image is presented in **B**, **C**, **D**, and **I**. Data are presented as the mean ± SEM (n = 3–5). $^{\#}P < 0.05$; $^{\#\#}P < 0.01$ by ANOVA with Tukey's HSD. $^{**}P < 0.005$; $^{***}P < 0.0005$ by two-tailed Student's *t* test

We next examined glucose tolerance and insulin resistance in TAZ P-KO mice under HFD conditions. Following the HFD, fasting blood glucose levels were markedly increased, and glucose intolerance was greatly aggravated in TAZ P-KO mice (Fig. 2E). At the same time, INS levels released by glucose stimulation was significantly lower in TAZ P-KO mice (Fig. 2F). Moreover, INS sensitivity was impaired in TAZ P-KO mice, as evidenced by persistent hyperglycemia even after INS injection (Fig. 2G). Histological analysis also confirmed that TAZ deficiency greatly increased lipid accumulation in adipose and liver tissues by HFD and exhibited irregularly shaped islets with aberrant INS and GCG expression (Fig. 2H). Isolated primary pancreatic islets were smaller, less dense, and more irregular in TAZ P-KO mice, particularly after HFD administration (Fig. 2I). INS levels secreted by glucose-stimulated islet cells were significantly decreased by TAZ deficiency (Fig. 2J). Although β-cell markers were significantly decreased in TAZ P-KO islet cells, other islet cell markers and inflammatory cytokines were substantially increased (Fig. 2K).

TAZ directly interacts with PDX1 in the pancreatic β-cells

We next attempted to elucidate the molecular mechanisms underlying INS production by TAZ. Since PDX1 and PAX6 are known to activate *INS* gene transcription [25, 44], we first assessed whether TAZ interacts with PDX1 and PAX6. The protein–protein interaction assay verified that TAZ was strongly associated with PDX1 but did not interact with PAX6 (Fig. 3A). We further identified specific interacting domains in TAZ and PDX1 using truncations of TAZ and PDX1 proteins. Although the C-terminal domain with or without WW domain failed to interact with PDX1, the N-terminal 123-amino acid (aa) region in TAZ was found to be essential for interaction with PDX1 (Fig. 3B). In addition, the N-terminal domain of PDX1 (1–139 aa) had no interaction with TAZ, but the region containing the homeodomain of PDX1 (140–240 aa) was associated with TAZ (Fig. 3C). More importantly, the endogenous TAZ formed a complex with PDX1 in pancreatic β-islet NIT-1 cells under high glucose conditions (Fig. 3D). Protein–protein interaction of endogenous TAZ and PDX1 was also verified in the pancreas of WT mice, not in the TAZ-deficient pancreas (Fig. 3E).

TAZ promotes INS gene transcription through induction of the transcriptional activity of PDX1

The direct interaction between PDX1 and TAZ prompted us to analyze its effect on *INS* gene promoter activity. Increased expression of PDX1 alone did not induce *INS* promoter activity in HEK293T cells; however, it dose-dependently increased the promoter activity in the presence of ectopic TAZ overexpression (Fig. 4A, B). Increasing amounts of TAZ also significantly promoted *INS* promoter activity only in the presence of PDX1, where PDX1 expression was unaffected by TAZ (Fig. 4C). The degradation-resistant TAZ mutant form (TAZ S4A) expressed a greater amount of TAZ and increased PDX1-induced *INS* promoter activity, stronger than WT TAZ (Fig. 4D). Interestingly, *INS* promoter activity was significantly increased by the ectopic PDX1, not PAX6, expression alone in mesenchymal stem-like C3H10T1/2 cells and further synergistically increased by TAZ overexpression (Fig. 4E). The N-terminal domain of TAZ (TAZ 1–123) selectively and sufficiently increased *INS* promoter activity in combination with PDX1 through interaction with PDX1 (Fig. 4F). Likewise, TAZ specifically increased *INS* promoter activity only in the presence of PDX1 truncations containing the homeodomain that interacts with
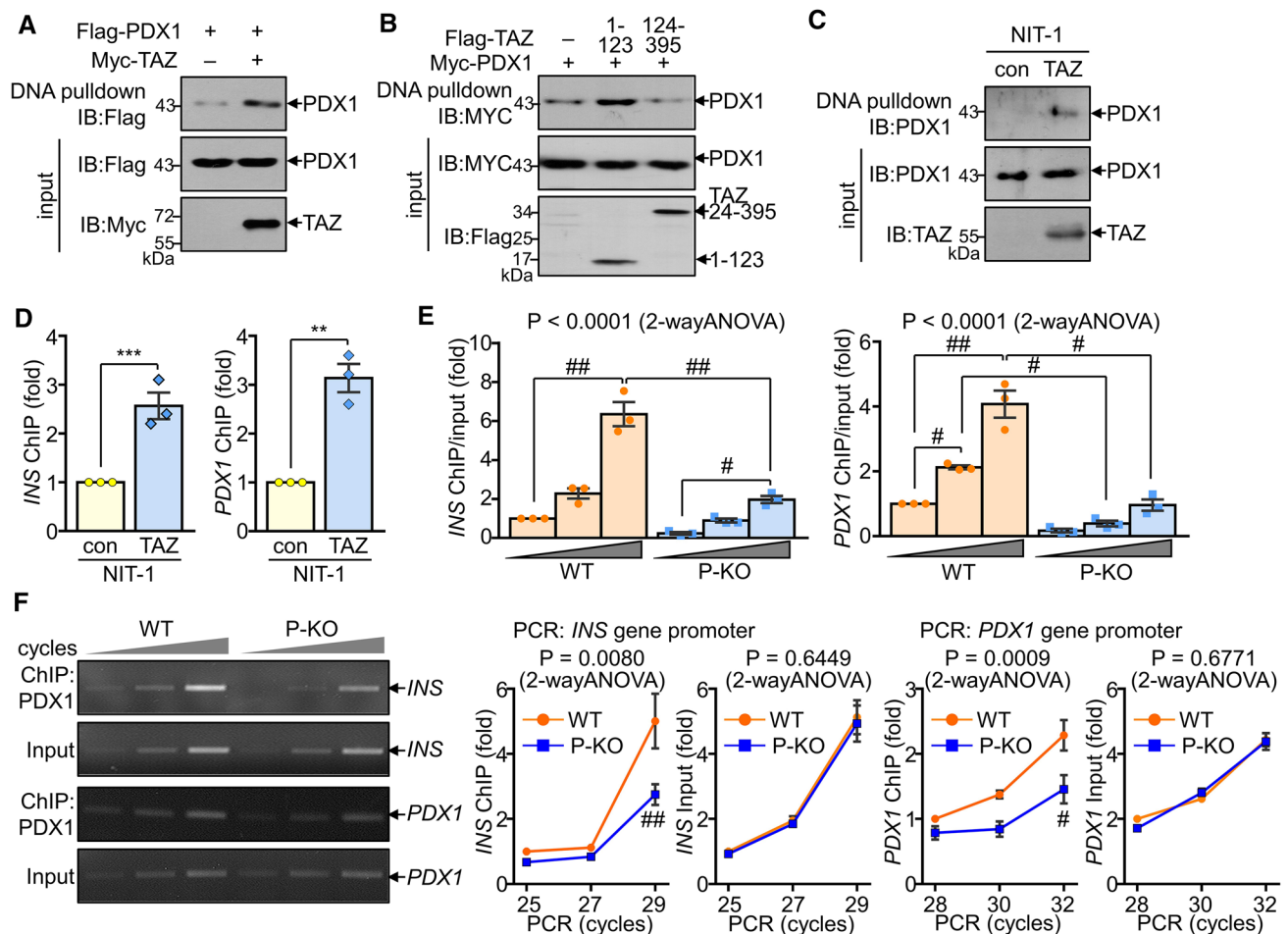
Fig. 5 Enhanced DNA-binding activity of PDX1 by TAZ. **A**, **B** HEK293T cells were transfected with Flag-PDX1 and 6xMyc-TAZ expression vector (**A**) or Flag-TAZ truncations and Myc-PDX1 (**B**) and harvested for DNA-pulldown assay. Protein extracts were incubated with biotinylated double-stranded insulin gene promoter DNA and subsequently streptavidin-conjugated agarose beads, followed by precipitation and immunoblot analysis. **C** Protein extracts were harvested from stable con/NIT-1 and TAZ/NIT-1 cells and subjected to DNA pulldown and immunoblot assay. **D** Chromatin DNA–protein complexes were harvested from stable con/NIT-1 and TAZ/NIT-1 cells and subjected to ChIP with anti-PDX1 antibody and subse-quent quantitative real-time PCR analysis. **E**, **F** Pancreatic islets were isolated from WT and TAZ P-KO mice and subjected to ChIP and quantitative real-time PCR analysis (**E**). ChIPed eluates and input were subjected to semi-quantitative PCR. The *INS* or *PDX1* gene promoter was amplified with the specific primer sets for different cycles of PCR reaction. Quantitative analysis was done by Image J software (**F**). All experiments were conducted at least three times. A representative image is presented in **A**–**C**, and **F**. Data in **D**–**F** are presented as the mean ± SEM. **$P < 0.005$; ***$P < 0.0005$ by two-tailed Student's *t* test. #$P < 0.05$; ##$P < 0.01$ by 2wayANOVA with Tukey's multiple comparisons

TAZ (Fig. 4G). We further evaluated the importance of the TAZ–PDX1 complex in *INS* production by pancreatic β-islet NIT-1 cells. Exogenous TAZ overexpression significantly increased *INS* promoter activity in NIT-1 cells combined with either endogenous or exogenous PDX1 expression. Meanwhile, PDX1 and TAZ expression did not affect *GCG* gene promoter activity (Fig. 4H). More importantly, the increase of *INS* promoter activity by TAZ was impaired in siPDX1/NIT-1 cells, which lost approximately 50% of endogenous PDX1 expression in NIT-1 cells (Fig. 4I, J).

TAZ enhances the DNA-binding activity of PDX1 to the *INS* gene promoter

Since TAZ was found to be essential for the transcriptional activity of PDX1 through direct interaction, we investigated the effect of TAZ on the DNA-binding activity of PDX1.

The DNA pulldown assay demonstrated that exogenous PDX1 bound to the *INS* gene promoter, which was increased by TAZ overexpression (Fig. 5A). The DNA-binding activity of PDX1 was significantly enhanced by the N-terminal 123-aa region of TAZ interacting with PDX1; however, it was not affected by the C-terminal domain of TAZ (124–395) (Fig. 5B). Endogenous PDX1 in β-islet NIT-1 cells was unable to bind to the *INS* gene promoter, which was thought to be due to the low expression of endogenous TAZ. Interestingly, endogenous PDX1 was bound to the *INS* gene promoter DNA in TAZ-stable NIT-1 cells expressing a considerable amount of TAZ (Fig. 5C). Additional ChIP analysis confirmed that the DNA-binding activity of PDX1 to the promoter of *INS* and *PDX1* genes was markedly increased in TAZ-stable NIT-1 cells compared to control cells (Fig. 5D). In contrast to TAZ overexpression, the binding of endogenous PDX1 to chromatin DNA was substantially attenuated in the pancreas of TAZ P-KO, as evidenced by the ChIP and quantitative real-time PCR analysis (Fig. 5E). Semiquantitative PCR with different cycles also demonstrated that the binding of endogenous PDX1 to the *INS* or *PDX1* gene promoter was substantially decreased by TAZ deficiency (Fig. 5F).

TAZ expression is essential for INS production by pancreatic β-cells

We further evaluated the importance of TAZ expression levels in INS production by β-cells using stable cells stably expressing TAZ or with TAZ knockdown. INS-producing rat insulinoma INS-1 cells were introduced with TAZ WT or a degradation-resistant mutant TAZ S4A, and forced TAZ expression was confirmed in TAZ S4A/INS-1 stable cells (Fig. 6A). Although little endogenous TAZ or PDX1 was detected in INS-1 cells, forced TAZ expression was observed mainly in the nucleus with increased endogenous PDX1 in high glucose-stimulated INS-1 cells (Fig. 6B). In TAZ stable cells, INS production was significantly increased by low and high glucose stimulation (Fig. 6C). Concomitantly, *INS* transcript levels were increased in TAZ/INS-1 cells stably expressing TAZ (Fig. 6D). In addition, TAZ stable (TAZ S4A/NIT-1) cells were established in mouse β-islet NIT-1 cells (Fig. 6E). TAZ expression significantly increased INS secretion and the expression of β-cell markers (Fig. 6F, G). On the other hand, the expression of β-cell markers and INS secretion were significantly reduced in TAZ-knockdown NIT-1 cells compared with control cells (Fig. 6H, I). As expected, high glucose decreased the phosphorylation of MST kinases and moderately increased TAZ expression by inhibiting S89-phosphorylation (Fig. 6J). Additional immunofluorescence staining clarified that TAZ expression and nuclear level were increased in INS-1 cells in response to high glucose (Fig. 6K). It was also confirmed that nuclear

expression of TAZ and PDX1 and their co-localization in the nucleus were profoundly increased in TAZ/NIT-1 cells after high glucose stimulation (Fig. 6L).

Enforced TAZ expression promotes mesenchymal stem cell differentiation into IPCs

Since pancreatic islets are generated from the differentiation of MSCs in vivo [45], we next assessed whether TAZ affects MSC differentiation into IPCs using MSC-like progenitor C3H10T1/2 cells and bone marrow-derived MSCs. We first established TAZ-expressing and TAZ-knockdown C3H10T1/2 cells and confirmed that exogenous PDX1 increased *INS* promoter activity in a TAZ-dependent manner in C3H10T1/2 cells (Fig. 7A, B). Stable cells expressing PDX1, TAZ, or PDX1/TAZ were additionally established and induced to differentiate into IPCs. Equal amounts of PDX1 and TAZ expression were verified in established stable cells (Fig. 7C). After IPCs differentiation through the three-stage method, transcript levels of *INS* and *PDX1* was significantly increased in IPCs introduced with PDX1 and TAZ together, compared to the IPCs transfected with mock control, PDX1, or TAZ (Fig. 7D). Moreover, INS secretion by IPCs was increased in culture supernatants of differentiated IPCs expressing PDX1 and more significantly increased in stable cells expressing both PDX1 and TAZ (Fig. 7E). The insulin stimulation index of differentiated IPCs was significantly improved by the expression of PDX1 and TAZ (Fig. 7F). In addition, MSCs obtained from WT, TAZ KO, and TAZ MSC-KO mice were induced to differentiate into IPCs, and the differentiated IPCs showed no significant difference in the insulin stimulation index (Fig. 7G). However, INS secretion was attenuated in TAZ-deleted IPCs, while no INS induction was observed in undifferentiated MSCs (Fig. 7H). Consistently, TAZ deletion in MSCs impaired the expression of *INS* and *PDX1* in differentiated IPCs (Fig. 7I). To see whether TAZ restores the impaired expression of β-cell markers in KO cells, WT and TAZ KO MSCs were transduced with TAZ-expressing viruses and induced to differentiate into IPCs. Enforced TAZ expression was confirmed by immunoblot analysis (Fig. 7J). Interestingly, forced expression of TAZ into KO cells significantly increased INS production after IPCs differentiation, as in WT cells (Fig. 7K). Likewise, β-cell markers such as *INS*, *PDX1*, and *Glut2* were substantially increased by TAZ expression in both WT and KO, whereas the increased transcript levels of *SMS* and *PAX6* by TAZ deficiency were oppositely decreased by TAZ expression to similar levels in WT and KO IPCs (Fig. 7L).
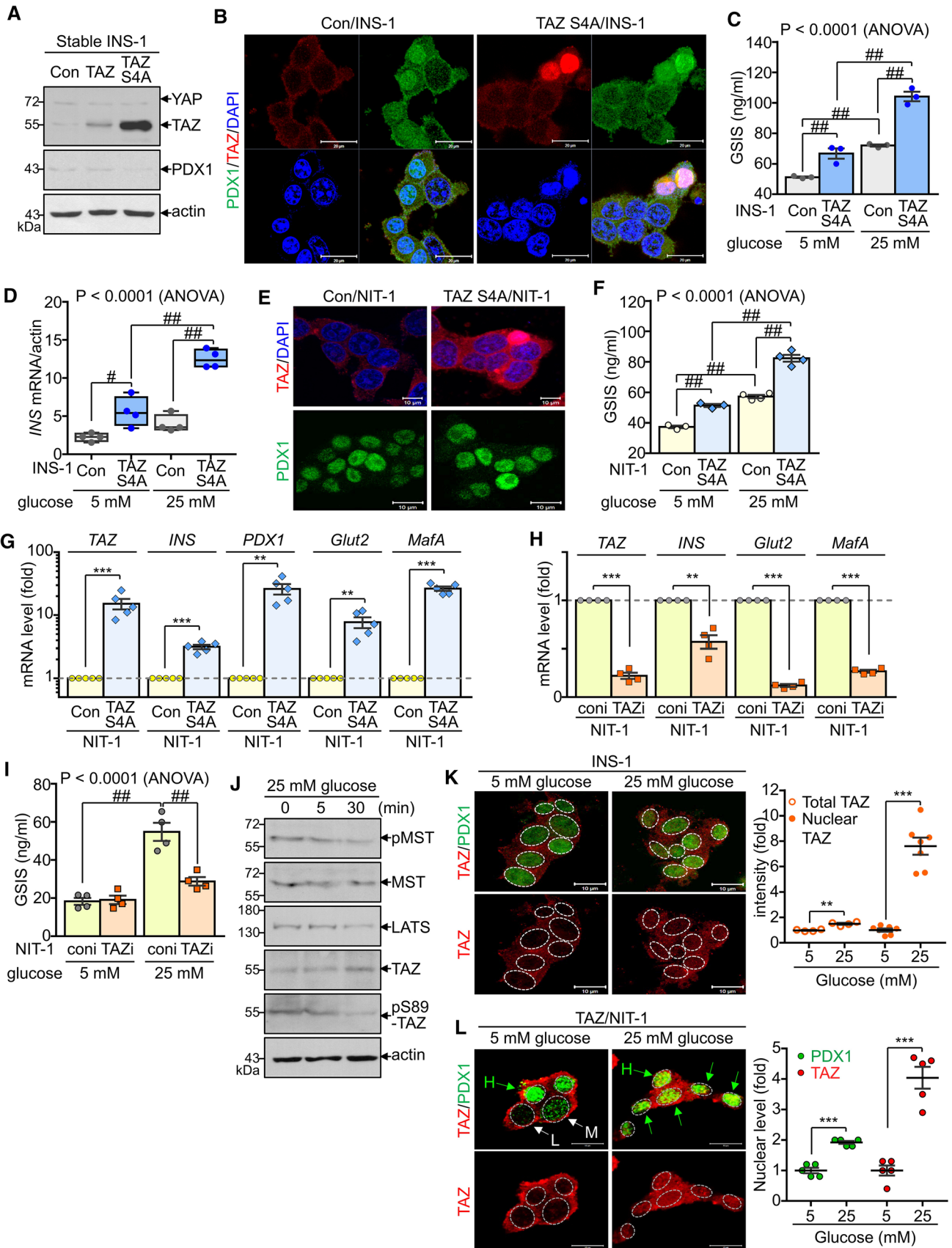
◄**Fig. 6** Increased insulin production by TAZ through glucose-mediated inhibition of the Hippo pathway in response to glucose. **A−C** Stable INS-1 cells expressing TAZ WT or S4A were established by retroviral transduction. TAZ expression was analyzed by immunoblot assay (**A**). Stable INS-1 cells were stained with antibodies against PDX1 and TAZ (**B**). Stable cells were maintained in glucose-free conditions for 2 h and stimulated with 5 mM and 25 mM glucose for 1 h, followed by INS ELISA (**C**). Stable cells were cultured under low glucose (5 mM) and high glucose (25 mM) conditions for 12 h and subjected to RT and quantitative real-time PCR analysis (**D**). **E−G** TAZ overexpressing cells (TAZ S4A/NIT-1) and the control cells (Con/NIT-1) were established in NIT-1 cells. Stable cells were stimulated with 25 mM glucose for 30 min for immunostaining of PDX1 and TAZ (**E**). Stable NIT-1 cells were subjected to GSIS assay following incubation with 25 mM glucose for 1 h (**F**). Cells were stimulated with 25 mM glucose for 12 h and subjected to quantitative analysis of β-cell markers (**G**). **H, I** TAZ knockdown cells (TAZi/NIT-1) and the respective control cells (coni/NIT-1) were established in NIT-1 cells. Cells were stimulated with 25 mM glucose for 12 h and subjected to determine relative transcript levels of *TAZ*, *INS*, *PDX1*, *Glut2*, and *MafA* (**H**). Cells were incubated with 25 mM glucose for 1 h for GSIS assay (**I**). **J** Pancreatic islet cells were isolated from WT ad TAZ P-KO mice and stimulated with 25 mM glucose for 1 h, followed by INS ELISA. **K−L** INS-1 cells were incubated in glucose-free RPMI-1640 medium for 6 h and treated with 25 mM glucose for the indicated times. Protein extracts were analyzed by immunoblot analysis (**K**). INS-1 cells were stimulated with 5 mM or 25 mM glucose for 30 min and immunostained with antibodies against TAZ and PDX1. The total intensity and nuclear intensity of TAZ were quantitatively calculated by Image J software (**L**). **M** TAZ stable NIT-1 cells were incubated in a glucose-free medium for 6 h and treated with 5 mM or 25 mM glucose for 30 min, followed by immunostaining. Nuclear levels of PDX1 and TAZ were quantitated by Image J software. A representative image out of at least three independent experiments is presented. Data are expressed as the mean ± SEM ($n = 3–6$). $^{\#}P < 0.05$; $^{\#\#}P < 0.01$ by ANOVA with Tukey's HSD test. $^{**}P < 0.005$; $^{***}P < 0.0005$ by two-tailed Student's *t* test

Discussion

TAZ is expressed in the pancreatic islets, and its deficiency alters pancreatic structure and function. High glucose increases INS production by pancreatic β-cells by activating TAZ through inhibition of the Hippo pathway and subsequently by promoting the DNA-binding and transcriptional activity of PDX1. TAZ also promotes IPCs differentiation from MSC, contributing to glucose homeostasis regulation. TAZ deficiency impairs INS production and causes hyperglycemia, leading to increased obesity and INS resistance (Fig. 8).

Maintaining INS-producing β-cell mass is important for glucose homeostasis [46]. The Hippo pathway coordinately regulates β-cell differentiation, proliferation, and apoptotic cell death, maintaining β-cell homeostasis [27]. It has been reported that deletion of MST1/2, the first component of the Hippo pathway, causes pancreatitis through immune cell infiltration [47, 48]. It has also been reported that MST1 is activated in diabetes, and its inhibition protects against β-cell apoptosis and restores β-cell function

in diabetes [49, 50]. Moreover, LATS2, another key Hippo pathway component, induces apoptotic cell death and dysfunction of β-cells, whereas its deficiency improves β-cell viability and INS secretion function [30]. Consistent with the improved β-cell function in the deficiency of MST and LATS, we also confirmed that enhanced TAZ activation resulting from the inhibition of MST kinases enhanced INS production by β-cell. However, sustained activation of YAP impairs pancreatic β-cell differentiation and function while YAP inhibition increases differentiation of stem cell-derived INS-producing β-cells [28, 29]. The TEAD family, the key transcription factor of the Hippo pathway, is important in maintaining cell proliferation, but it is also essential for maintaining β-cell identity through direct activation of β-cell markers, and its deficiency develops diabetes due to the lack of INS secretion [27, 51]. Despite these complex and contradictory results, it is clear that the Hippo signaling pathway is important for regulating pancreatic β-cell function. It also implies that Hippo mediators transduce the optimized signal required to control the balance of β-cell differentiation and proliferation through different molecular interactions and mechanisms. The finding that the pancreas-specific TAZ deletion did not alter YAP expression in the pancreas but resulted in decreased INS secretion and hyperglycemia clarified that TAZ plays an independent function different from YAP. Unlike YAP regulates TEAD activity and subsequently induces β-cell proliferation and survival, TAZ more likely increases PDX1 activity and promotes β-cell differentiation and function through interaction with TEAD and PDX1 [51]. It will be interesting to identify whether and how TAZ selects PDX1 and TEAD as its partner for inducing INS. TAZ may be an essential and beneficial target for regulating glucose homeostasis by increasing INS production in response to high glucose. In addition to alterations in β-cells, dysregulated Hippo pathway causes aberrant pancreatic acinar differentiation and pancreatic cancer development [47, 52, 53]. Altered pancreatic architecture in TAZ deficiency, including decreased islets, misplaced α-cells, and damaged epithelial cells, are similar to the aberrant pancreatic architecture caused by defective Hippo signaling [33]. Apart from the functional mechanisms of TAZ in pancreatic cancer development, it would be interesting to elucidate the detailed molecular mechanisms by which TAZ contributes to maintaining the pancreatic architecture.

Progressive β-cell loss from autoimmune attack leads to chronic hyperglycemia and increases the prevalence of obesity in type 1 diabetes (T1D); furthermore, obesity-induced hyperglycemia contributes to and exacerbates INS resistance, which is an important clinical feature of type 2 diabetes (T2D) [54, 55]. The prevalence of double diabetes (DD) or hybrid diabetes, a combination of INS resistance and autoimmune destruction of the INS-producing β-cells, has increased worldwide in youth onset diabetes [56, 57].
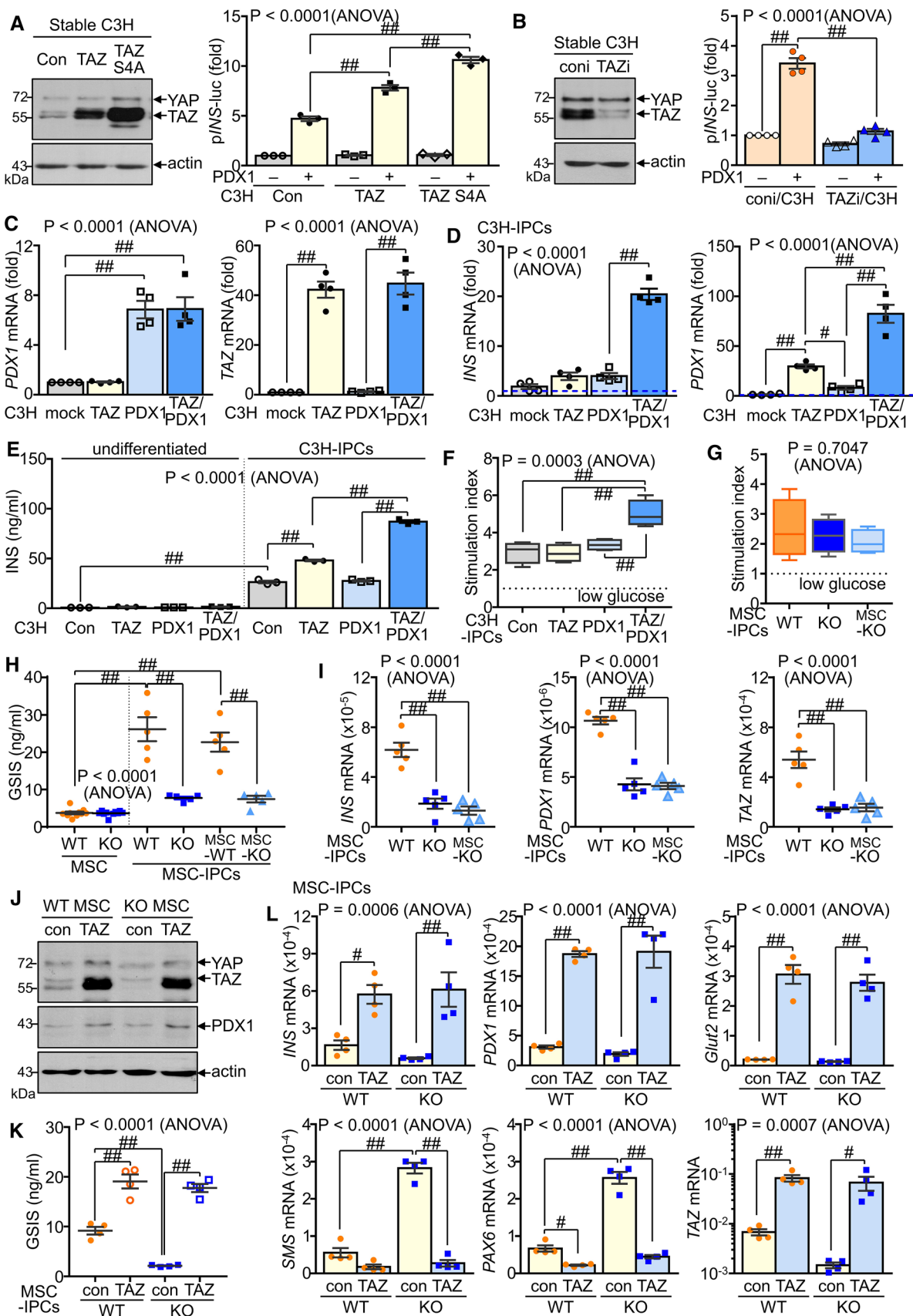
◄**Fig. 7** Promoted IPC differentiation by TAZ. **A** Stable C3H10T1/2 cells expressing TAZ WT or S4A were transfected with the p*INS*-luc reporter and PDX1 expression vector. The immunoblot analyzed TAZ expression, and the p*INS*-luc promoter activity was assessed by reporter assay. **B** Stable TAZ knockdown cells (TAZi/C3H) were established and transfected with the p*INS*-luc reporter and PDX1 expression vector. **C−E** Stable cells expressing PDX1, TAZ, and PDX1/TAZ were established in C3H10T1/2 cells and induced to differentiate into IPCs via three-stage methods. Relative transcripts of PDX1 and TAZ were analyzed in undifferentiated stable cells (**C**). Relative transcript levels of *INS* and *PDX1* were determined in IPCs at differentiation day 7 of stage 3 (**D**). Undifferentiated cells and differentiated IPCs were cultured in 25 mM glucose for 24 h, and supernatants were subjected to INS ELISA (**E**). Differentiated IPCs were stimulated with 25 mM glucose for 1 h after glucose deprivation for 2 h, followed by INS ELISA. The stimulation index was calculated by dividing INS levels at 25 mM glucose with INS released at 5 mM glucose (**F**). **G−I** MSCs were isolated from the bone marrow of WT, TAZ KO, and TAZ Prrx1-KO (MSC-KO) mice and induced to differentiate into IPCs. The stimulation index was determined by measuring secreted INS at 5 mM and 25 mM glucose (**G**). MSCs and differentiated IPCs were stimulated with 25 mM glucose for 1 h for GSIS assay (**H**). Differentiated IPCs were harvested and subjected to quantitative real-time PCR analysis (**I**). **J−L** WT and TAZ KO MSCs were transfected with TAZ-expressing viruses and induced to differentiate into IPCs. TAZ and PDX1 expression were analyzed by immunoblot assay (**J**). IPCs were stimulated with 25 mM glucose for 1 h after glucose deprivation, followed by INS ELISA (**K**). IPCs were stimulated with 25 mM glucose for 12 h and harvested to determine relative transcript levels of islet markers (**L**). All experiments were conducted at least three times, and a representative image is presented in **A**, **B**, and **J**. Data are expressed as the mean ± SEM ($n = 3$–5). $^{#}P < 0.05$; $^{##}P < 0.01$ by ANOVA with Tukey's HSD test

In addition, older adults with T1D are also at an increased risk for developing severe hyperglycemia and INS resistance, strongly suggesting the importance and necessity of developing therapeutics for DD [54, 58]. The TAZ genetic defect in the pancreas causes hyperglycemia, increases the prevalence of ageing- or HFD-related obesity, and exacerbates HFD-induced INS resistance. Therefore, it is suggested that TAZ P-KO mice are useful for developing and evaluating DD therapeutics. Various therapeutic strategies have been developed to treat diabetes, including INS delivery, immunotherapy, and β-cell replacement [59]. Some or all of INS-producing β-cells are destroyed in the pancreas in T1D, leaving the patient with little or no INS and too much glucose in the bloodstream. Thus, transplantation of IPCs is considered the most promising therapeutic strategy; however, this strategy has limitations in terms of poor viability after transplantation [59]. Therefore, it will be important to study whether TAZ gene delivery to human islet cells or MSCs can improve cell transplantation efficiency, potentiate INS-secreting β-cell function, and attenuate complications for treating T1D. Since TAZ promotes muscle cell differentiation and increases INS sensitivity in muscle cells [60, 61], TAZ-delivered MSCs therapeutics may have dual beneficial effects in diabetes by increasing INS secretion and INS sensitivity in vivo. In addition, pharmacological approaches to activate endogenous TAZ in the pancreas may prevent and treat T1D, T2D, and DD.
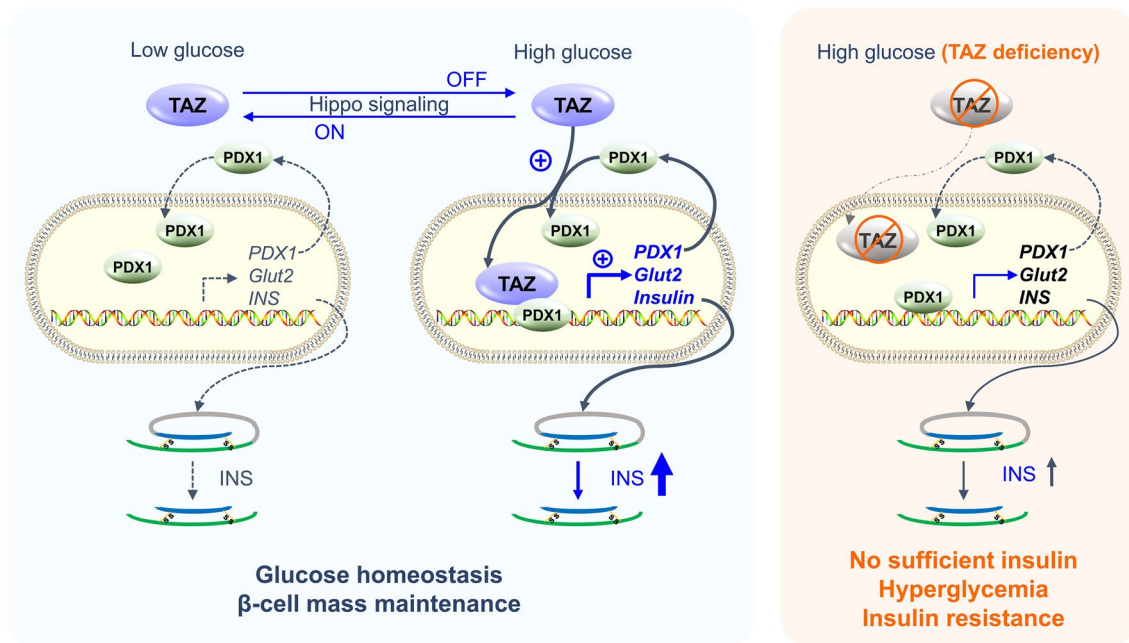

Fig. 8 Modulation of insulinogenesis in pancreatic β-cells by a Hippo mediator, TAZ. The hippo pathway transduces on/off signaling to modulate INS by pancreatic β-cells in response to glucose concentration. TAZ activation following Hippo off signaling in response to high glucose promotes INS production through cooperation with PDX1, leading to regulation of glucose homeostasis. However, TAZ deficiency fails to increase the DNA-binding and transcriptional activity of PDX1, which reduces INS production and impairs glucose homeostasis. The persistent failure of glucose homeostasis in TAZ deficiency also results in INS resistance upon ageing and obesity

Indeed, the TAZ activator TM25659 has been reported to improve HFD-induced hyperglycemia and INS resistance in mice [38, 62], indicating the potential of TAZ in the prevention and treatment of metabolic diseases.

Data availability No datasets were generated during the current study, and all data are provided in full in the results section of this paper.

Declarations

Conflict of interest The authors declare no competing interests regarding this manuscript.

Ethical standards All animal care and experiments were approved by the International Animal Care and Use Committee (IACUC; 2010-13-3, 2015-01-020, 17-013, and 19-031) at Ewha Womans University and were conducted according to the IACUC guidelines. The study was performed in accordance with the Declaration of Helsinki.

References

1. Hong JH, Hwang ES, McManus MT, Amsterdam A, Tian Y, Kalmukova R, Mueller E, Benjamin T, Spiegelman BM, Sharp PA, Hopkins N, Yaffe MB (2005) TAZ, a transcriptional modulator of mesenchymal stem cell differentiation. Science 309:1074–1078. https://doi.org/10.1126/science.1110955
2. Jeong H, Bae S, An SY, Byun MR, Hwang JH, Yaffe MB, Hong JH, Hwang ES (2010) TAZ as a novel enhancer of MyoD-mediated myogenic differentiation. FASEB J 24:3310–3320. https://doi.org/10.1096/fj.09-151324
3. Jeong MG, Kim HK, Hwang ES (2021) The essential role of TAZ in normal tissue homeostasis. Arch Pharm Res 44:253–262. https://doi.org/10.1007/s12272-021-01322-w
4. Jang EJ, Jeong H, Han KH, Kwon HM, Hong JH, Hwang ES (2012) TAZ suppresses NFAT5 activity through tyrosine phosphorylation. Mol Cell Biol 32:4925–4932. https://doi.org/10.1128/MCB.00392-12
5. Jeong MG, Song H, Shin JH, Jeong H, Kim HK, Hwang ES (2017) Transcriptional co-activator with PDZ-binding motif is required to sustain testicular function on aging. Aging Cell 16:1035–1042. https://doi.org/10.1111/acel.12631
6. Shin JH, Lee G, Jeong MG, Kim HK, Won HY, Choi Y, Lee JH, Nam M, Choi CS, Hwang GS, Hwang ES (2020) Transcriptional co-activator with PDZ-binding motif suppresses the expression of steroidogenic enzymes by nuclear receptor 4 A1 in Leydig cells. FASEB J 34:5332–5347. https://doi.org/10.1096/fj.201900695RRRR
7. Lin KC, Park HW, Guan KL (2017) Regulation of the Hippo pathway transcription factor TEAD. Trends Biochem Sci 42:862–872. https://doi.org/10.1016/j.tibs.2017.09.003
8. Holden JK, Cunningham CN (2018) Targeting the Hippo pathway and cancer through the TEAD family of transcription factors. Cancers (Basel). https://doi.org/10.3390/cancers10030081
9. Konishi T, Schuster RM, Lentsch AB (2018) Proliferation of hepatic stellate cells, mediated by YAP and TAZ, contributes to liver repair and regeneration after liver ischemia/reperfusion injury. Am J Physiol Gastrointest Liver Physiol 314:G471–G482. https://doi.org/10.1152/ajpgi.00153.2017
10. Yui S, Azzolin L, Maimets M, Pedersen MT, Fordham RP, Hansen SL, Larsen HL, Guiu J, Alves MRP, Rundsten CF, Johansen JV, Li Y, Madsen CD, Nakamura T, Watanabe M, Nielsen OH, Schweiger PJ, Piccolo S, Jensen KB (2018) YAP/TAZ-dependent reprogramming of colonic epithelium links ECM remodeling to tissue regeneration. Cell Stem Cell 22:35-49 e37. https://doi.org/10.1016/j.stem.2017.11.001
11. Kim AR, Park JI, Oh HT, Kim KM, Hwang JH, Jeong MG, Kim EH, Hwang ES, Hong JH (2019) TAZ stimulates liver regeneration through interleukin-6-induced hepatocyte proliferation and inhibition of cell death after liver injury. FASEB J 33:5914–5923. https://doi.org/10.1096/fj.201801256RR
12. Zhang H, Liu CY, Zha ZY, Zhao B, Yao J, Zhao S, Xiong Y, Lei QY, Guan KL (2009) TEAD transcription factors mediate the function of TAZ in cell growth and epithelial-mesenchymal transition. J Biol Chem 284:13355–13362. https://doi.org/10.1074/jbc.M900843200
13. Chan SW, Lim CJ, Guo K, Ng CP, Lee I, Hunziker W, Zeng Q, Hong W (2008) A role for TAZ in migration, invasion, and tumorigenesis of breast cancer cells. Cancer Res 68:2592–2598. https://doi.org/10.1158/0008-5472.CAN-07-2696
14. Zhou Z, Hao Y, Liu N, Raptis L, Tsao MS, Yang X (2011) TAZ is a novel oncogene in non-small cell lung cancer. Oncogene 30:2181–2186. https://doi.org/10.1038/onc.2010.606
15. Bartucci M, Dattilo R, Moriconi C, Pagliuca A, Mottolese M, Federici G, Benedetto AD, Todaro M, Stassi G, Sperati F, Amabile MI, Pilozzi E, Patrizii M, Biffoni M, Maugeri-Sacca M, Piccolo S, De Maria R (2015) TAZ is required for metastatic activity and chemoresistance of breast cancer stem cells. Oncogene 34:681–690. https://doi.org/10.1038/onc.2014.5
16. Pocaterra A, Romani P, Dupont S (2020) YAP/TAZ functions and their regulation at a glance. J Cell Sci. https://doi.org/10.1242/jcs.230425
17. Da Silva Xavier G (2018) The cells of the Islets of Langerhans. J Clin Med. https://doi.org/10.3390/jcm7030054
18. Lee EK, Gorospe M (2010) Minireview: posttranscriptional regulation of the insulin and insulin-like growth factor systems. Endocrinology 151:1403–1408. https://doi.org/10.1210/en.2009-1123
19. Docherty HM, Hay CW, Ferguson LA, Barrow J, Durward E, Docherty K (2005) Relative contribution of PDX-1, MafA and E47/beta2 to the regulation of the human insulin promoter. Biochem J 389:813–820. https://doi.org/10.1042/BJ20041891
20. Gannon M, Ables ET, Crawford L, Lowe D, Offield MF, Magnuson MA, Wright CV (2008) Pdx-1 function is specifically required in embryonic beta cells to generate appropriate numbers of endocrine cell types and maintain glucose homeostasis. Dev Biol 314:406–417. https://doi.org/10.1016/j.ydbio.2007.10.038
21. Gao T, McKenna B, Li C, Reichert M, Nguyen J, Singh T, Yang C, Pannikar A, Doliba N, Zhang T, Stoffers DA, Edlund H, Matschinsky F, Stein R, Stanger BZ (2014) Pdx1 maintains beta cell identity and function by repressing an alpha cell program. Cell Metab 19:259–271. https://doi.org/10.1016/j.cmet.2013.12.002

22. Taylor BL, Liu FF, Sander M (2013) Nkx6.1 is essential for maintaining the functional state of pancreatic beta cells. Cell Rep 4:1262–1275. https://doi.org/10.1016/j.celrep.2013.08.010

23. Thorens B (2015) GLUT2, glucose sensing and glucose homeostasis. Diabetologia 58:221–232. https://doi.org/10.1007/s00125-014-3451-1

24. Lantz KA, Vatamaniuk MZ, Brestelli JE, Friedman JR, Matschinsky FM, Kaestner KH (2004) Foxa2 regulates multiple pathways of insulin secretion. J Clin Investig 114:512–520. https://doi.org/10.1172/JCI21149

25. Gosmain Y, Katz LS, Masson MH, Cheyssac C, Poisson C, Philippe J (2012) Pax6 is crucial for beta-cell function, insulin biosynthesis, and glucose-induced insulin secretion. Mol Endocrinol 26:696–709. https://doi.org/10.1210/me.2011-1256

26. Ardestani A, Lupse B, Maedler K (2018) Hippo signaling: key emerging pathway in cellular and whole-body metabolism. Trends Endocrinol Metab 29:492–509. https://doi.org/10.1016/j.tem.2018.04.006

27. Ardestani A, Maedler K (2018) The Hippo signaling pathway in pancreatic beta-cells: functions and regulations. Endocr Rev 39:21–35. https://doi.org/10.1210/er.2017-00167

28. Rosado-Olivieri EA, Anderson K, Kenty JH, Melton DA (2019) YAP inhibition enhances the differentiation of functional stem cell-derived insulin-producing beta cells. Nat Commun 10:1464. https://doi.org/10.1038/s41467-019-09404-6

29. Yuan T, Rafizadeh S, Azizi Z, Lupse B, Gorrepati KDD, Awal S, Oberholzer J, Maedler K, Ardestani A (2016) Proproliferative and antiapoptotic action of exogenously introduced YAP in pancreatic beta cells. JCI Insight 1:e86326. https://doi.org/10.1172/jci.insight.86326

30. Yuan T, Annamalai K, Naik S, Lupse B, Geravandi S, Pal A, Dobrowolski A, Ghawali J, Ruhlandt M, Gorrepati KDD, Azizi Z, Lim DS, Maedler K, Ardestani A (2021) The Hippo kinase LATS2 impairs pancreatic beta-cell survival in diabetes through the mTORC1-autophagy axis. Nat Commun 12:4928. https://doi.org/10.1038/s41467-021-25145-x

31. Morvaridi S, Dhall D, Greene MI, Pandol SJ, Wang Q (2015) Role of YAP and TAZ in pancreatic ductal adenocarcinoma and in stellate cells associated with cancer and chronic pancreatitis. Sci Rep 5:16759. https://doi.org/10.1038/srep16759

32. Gruber R, Panayiotou R, Nye E, Spencer-Dene B, Stamp G, Behrens A (2016) YAP1 and TAZ control pancreatic cancer initiation in mice by direct up-regulation of JAK-STAT3 signaling. Gastroenterology 151:526–539. https://doi.org/10.1053/j.gastro.2016.05.006

33. Wu Y, Aegerter P, Nipper M, Ramjit L, Liu J, Wang P (2021) Hippo signaling pathway in pancreas development. Front Cell Dev Biol 9:663906. https://doi.org/10.3389/fcell.2021.663906

34. Freemark M, Avril I, Fleenor D, Driscoll P, Petro A, Opara E, Kendall W, Oden J, Bridges S, Binart N, Breant B, Kelly PA (2002) Targeted deletion of the PRL receptor: effects on islet development, insulin production, and glucose tolerance. Endocrinology 143:1378–1385. https://doi.org/10.1210/endo.143.4.8722

35. Krishnamurthy M, Ayazi F, Li J, Lyttle AW, Woods M, Wu Y, Yee SP, Wang R (2007) c-Kit in early onset of diabetes: a morphological and functional analysis of pancreatic beta-cells in c-KitW-v mutant mice. Endocrinology 148:5520–5530. https://doi.org/10.1210/en.2007-0387

36. Rao X, Huang X, Zhou Z, Lin X (2013) An improvement of the $2^{(-\text{delta delta CT})}$ method for quantitative real-time polymerase chain reaction data analysis. Biostat Bioinform Biomath 3:71–85

37. Vinue A, Gonzalez-Navarro H (2015) Glucose and insulin tolerance tests in the mouse. Methods Mol Biol 1339:247–254. https://doi.org/10.1007/978-1-4939-2929-0_17

38. Jung JG, Yi SA, Choi SE, Kang Y, Kim TH, Jeon JY, Bae MA, Ahn JH, Jeong H, Hwang ES, Lee KW (2015) TM-25659-induced activation of fgf21 level decreases insulin resistance and inflammation in skeletal muscle via GCN2 pathways. Mol Cells 38:1037–1043. https://doi.org/10.14348/molcells.2015.0100

39. Li DS, Yuan YH, Tu HJ, Liang QL, Dai LJ (2009) A protocol for islet isolation from mouse pancreas. Nat Protoc 4:1649–1652. https://doi.org/10.1038/nprot.2009.150

40. Kim TH, Kim HK, Hwang ES (2017) Novel anti-adipogenic activity of anti-malarial amodiaquine through suppression of PPAR-gamma activity. Arch Pharm Res 40:1336–1343. https://doi.org/10.1007/s12272-017-0965-3

41. Gabr MM, Sobh MM, Zakaria MM, Refaie AF, Ghoneim MA (2008) Transplantation of insulin-producing clusters derived from adult bone marrow stem cells to treat diabetes in rats. Exp Clin Transplant 6:236–243. https://doi.org/10.3727/096368910X522270

42. Czubak P, Bojarska-Junak A, Tabarkiewicz J, Putowski L (2014) A modified method of insulin producing cells' generation from bone marrow-derived mesenchymal stem cells. J Diabetes Res 2014:628591. https://doi.org/10.1155/2014/628591

43. Legro RS, Finegood D, Dunaif A (1998) A fasting glucose to insulin ratio is a useful measure of insulin sensitivity in women with polycystic ovary syndrome. J Clin Endocrinol Metab 83:2694–2698. https://doi.org/10.1210/jcem.83.8.5054

44. Ahlgren U, Jonsson J, Jonsson L, Simu K, Edlund H (1998) Beta-cell-specific inactivation of the mouse Ipf1/Pdx1 gene results in loss of the beta-cell phenotype and maturity onset diabetes. Genes Dev 12:1763–1768. https://doi.org/10.1101/gad.12.12.1763

45. Zhang Y, Dou Z (2014) Under a nonadherent state, bone marrow mesenchymal stem cells can be efficiently induced into functional islet-like cell clusters to normalize hyperglycemia in mice: a control study. Stem Cell Res Ther 5:66. https://doi.org/10.1186/scrt455

46. Rutter GA, Pullen TJ, Hodson DJ, Martinez-Sanchez A (2015) Pancreatic beta-cell identity, glucose sensing and the control of insulin secretion. Biochem J 466:203–218. https://doi.org/10.1042/BJ20141384

47. Gao T, Zhou D, Yang C, Singh T, Penzo-Mendez A, Maddipati R, Tzatsos A, Bardeesy N, Avruch J, Stanger BZ (2013) Hippo signaling regulates differentiation and maintenance in the exocrine pancreas. Gastroenterology 144:1543–1553, e1541. https://doi.org/10.1053/j.gastro.2013.02.037

48. George NM, Day CE, Boerner BP, Johnson RL, Sarvetnick NE (2012) Hippo signaling regulates pancreas development through inactivation of Yap. Mol Cell Biol 32:5116–5128. https://doi.org/10.1128/MCB.01034-12

49. Ardestani A, Tremblay MS, Shen W, Maedler K (2019) Neratinib is an MST1 inhibitor and restores pancreatic beta-cells in diabetes. Cell Death Discov 5:149. https://doi.org/10.1038/s41420-019-0232-0

50. Ardestani A, Paroni F, Azizi Z, Kaur S, Khobragade V, Yuan T, Frogne T, Tao W, Oberholzer J, Pattou F, Conte JK, Maedler K (2014) MST1 is a key regulator of beta cell apoptosis and dysfunction in diabetes. Nat Med 20:385–397. https://doi.org/10.1038/nm.3482

51. Lee J, Liu R, Kim BS, Zhang Y, Li F, Jagannathan R, Yang P, Negi V, Perez-Garcia EM, Saha PK, Sabek O, Coarfa C, Creighton CJ, Huising MO, Bottino R, Ma K, Moulik M, Yechoor VK (2020) Tead1 reciprocally regulates adult β-cell proliferation and function to maintain glucose homeostasis. bioRxiv. https://doi.org/10.1101/2020.03.05.979450

52. Liu J, Gao M, Nipper M, Deng J, Sharkey FE, Johnson RL, Crawford HC, Chen Y, Wang P (2019) Activation of the intrinsic fibro-inflammatory program in adult pancreatic acinar cells triggered

by Hippo signaling disruption. PLoS Biol 17:e3000418. https://doi.org/10.1371/journal.pbio.3000418

53. Ansari D, Ohlsson H, Althini C, Bauden M, Zhou Q, Hu D, Andersson R (2019) The Hippo signaling pathway in pancreatic cancer. Anticancer Res 39:3317–3321. https://doi.org/10.21873/anticanres.13474

54. Czech MP (2017) Insulin action and resistance in obesity and type 2 diabetes. Nat Med 23:804–814. https://doi.org/10.1038/nm.4350

55. Corbin KD, Driscoll KA, Pratley RE, Smith SR, Maahs DM, Mayer-Davis EJ, Advancing Care for Type 1 Diabetes and Obesity Network (2018) Obesity in type 1 diabetes: pathophysiology, clinical impact, and mechanisms. Endocr Rev 39:629–663. https://doi.org/10.1210/er.2017-00191

56. Pozzilli P, Buzzetti R (2007) A new expression of diabetes: double diabetes. Trends Endocrinol Metab 18:52–57. https://doi.org/10.1016/j.tem.2006.12.003

57. Khawandanah J (2019) Double or hybrid diabetes: a systematic review on disease prevalence, characteristics and risk factors. Nutr Diabetes 9:33. https://doi.org/10.1038/s41387-019-0101-1

58. Polsky S, Ellis SL (2015) Obesity, insulin resistance, and type 1 diabetes mellitus. Curr Opin Endocrinol Diabetes Obes 22:277–282. https://doi.org/10.1097/MED.0000000000000170

59. Pathak V, Pathak NM, O'Neill CL, Guduric-Fuchs J, Medina RJ (2019) Therapies for type 1 diabetes: current scenario and future perspectives. Clin Med Insights Endocrinol Diabetes 12:1179551419844521. https://doi.org/10.1177/1179551419844521

60. Hwang JH, Kim AR, Kim KM, Il Park J, Oh HT, Moon SA, Byun MR, Jeong H, Kim HK, Yaffe MB, Hwang ES, Hong JH (2019) TAZ couples Hippo/Wnt signalling and insulin sensitivity through Irs1 expression. Nat Commun 10:421. https://doi.org/10.1038/s41467-019-08287-x

61. Park GH, Jeong H, Jeong MG, Jang EJ, Bae MA, Lee YL, Kim NJ, Hong JH, Hwang ES (2014) Novel TAZ modulators enhance myogenic differentiation and muscle regeneration. Br J Pharmacol 171:4051–4061. https://doi.org/10.1111/bph.12755

62. Jang EJ, Jeong H, Kang JO, Kim NJ, Kim MS, Choi SH, Yoo SE, Hong JH, Bae MA, Hwang ES (2012) TM-25659 enhances osteogenic differentiation and suppresses adipogenic differentiation by modulating the transcriptional co-activator TAZ. Br J Pharmacol 165:1584–1594. https://doi.org/10.1111/j.1476-5381.2011.01664.x